Deformable Hollow Hybrid Silica/Siloxane Colloids by Emulsion Templating

Carmen I. Zoldesi,*,† Cornelis A. van Walree,‡ and Arnout Imhof*,†

Soft Condensed Matter, Debye Institute, Utrecht University, Princetonplein 5, 3584 CC Utrecht, The Netherlands, and Organic Chemistry and Catalysis, Debye Institute, Utrecht University, Padualaan 8, 3584 CH, The Netherlands

Received January 11, 2006. In Final Form: March 1, 2006

A procedure to obtain hollow colloidal particles has been developed using an emulsion templating technique. Monodisperse silicone oil droplets were prepared by hydrolysis and polymerization of dimethyldiethoxysilane monomer and incorporated in a solid shell using tetraethoxysilane. Hollow shells were obtained by exchange of the core. The formation of the oil droplets was investigated using static light scattering and ^{29}Si solution NMR, and the hollow shells were characterized by electron microscopy and static light scattering. Details on the composition of the shell material were obtained from energy-dispersive X-ray analysis and ^{29}Si solid state NMR, revealing that the shells consist of a hybrid cross-linked network of silica and siloxane units. Confocal microscopy was used to show that the shells are permeable to small dye molecules. The thickness of the coating can be easily varied from a few nanometers upward. Depending on the ratio of shell thickness to particle radius, three types of hollow shells can be distinguished depending on the way in which they buckle upon drying. We designate them as microspheres, microcapsules, and microballoons. As a result of their monodispersity, these particles can be used for making 3D-ordered materials.

Introduction

Synthesis of new types of colloidal particles represents an intense and rapidly developing field of research because of their potential use in a variety of applications. They are attractive as building blocks for ordered and complex materials but also for chemical engineering and pharmaceutical and biological purposes. Among them, hollow colloidal particles represent a distinct class of colloids with additional applications in molecular transport, encapsulation, controlled storage and release, catalysis, and manufacturing of highly porous materials.

The procedure to make hollow colloids usually involves preparation of core−shell particles, followed by removal of the cores. Such hybrid particles can often be prepared by controlled precipitation of inorganic precursors onto the core particles. A different approach is to deposit small particles of the coating material onto the cores. This is done, for example, in the layer-by-layer technique, in which case successive layers of anionic particles were deposited, alternated by layers of cationic polymer.[1−3]

A variety of templating agents has been used in the synthesis of hollow spheres: latex,[2,4−6] silica,[7−10] gold,[11] or zinc sulfide colloidal particles.[12] If desired, the template can be removed by dissolution of the core (in the case of silica, gold, or zinc sulfide) or heating (for latex cores).

Because of limitations related to their polydispersity or difficulties concerning the coating procedures, a considerably smaller number of methods have used liquid cores as templates for the coating. These were either emulsion droplets[13−15] or vesicles.[16−19]

Depending on the type of coating, the resulting hollow shells have been made of very diverse materials, from silica,[2,6,13−15,18] gold,[7,20] and titania[4] to organic polymers,[8−11,17,21] polyelectrolytes,[19] and their hybrids.[22] Composite particles of high-molecular weight silicone oil and silica were made, but without a core−shell structure.[23]

We recently reported a facile method for preparing monodisperse hollow colloidal particles, based on an emulsion templating technique.[24] The basic idea of our method is to prepare highly uniform silicone oil-in-water emulsion droplets by hydrolysis and polymerization of dimethyldiethoxysilane[25] and to use them as templates around which a solid material is grown by hydrolysis and condensation of tetraethoxysilane. Earlier

* Corresponding authors. E-mails: c.i.zoldesi@phys.uu.nl (C.I.Z.) and a.imhof@phys.uu.nl (A.I.).

† Soft Condensed Matter.

‡ Organic Chemistry and Catalysis.

(1) Caruso, F.; Lichtenfeld, H.; Giersig, M.; Mohwald, H. *J. Am. Chem. Soc.* **1998**, *120*, 8523.
(2) Caruso, F.; Caruso, R. A.; Mohwald, H. *Science* **1998**, *282*, 1111.
(3) Yin, Y.; Lu, Y.; Gates, B.; Xia, Y. *Chem. Mater.* **2001**, *13*, 1146.
(4) Imhof, A. *Langmuir* **2001**, *17*, 3579.
(5) Caruso, F. *Adv. Mater.* **2001**, *13*, 11.
(6) Cornelissen, J. J. L. M.; Connor, E. F.; Kim, H.-C.; Lee, V. Y.; Magibitang, T.; Rice, P. M.; Volksen, W.; Sundberg, L. K.; Miller, R. D. *Chem. Commun.* **2003**, 1010.
(7) Graf, C.; van Blaaderen, A. *Langmuir* **2002**, *18*, 524.
(8) Zha, L.; Zhang, Y.; Yang, W.; Fu, S. *Adv. Mater.* **2002**, *14*, 1090.
(9) Mandal, T. K.; Fleming, M. S.; Walt, D. R. *Chem. Mater.* **2000**, *12*, 3481.
(10) Xu, X.; Asher, S. A. *J. Am. Chem. Soc.* **2004**, *126*, 7940.
(11) Marinakos, S. M.; Shultz, D. A.; Feldheim, D. L. *Adv. Mater.* **1999**, *11*, 34.
(12) Velikov, K. P.; van Blaaderen, A. *Langmuir* **2001**, *17*, 4779.
(13) Sun, Q.; Kooyman, P. J.; Grossmann, J. G.; Bomans, P. H. H.; Frederik, P. M.; Magusin, P. C. M. M.; Beelen, T. P. M.; van Santen, R. A.; Sommerdijk, N. A. J. M. *Adv. Mater.* **2003**, *15*, 1097.
(14) Jafelicci, M., Jr.; Davolos, M. R.; dos Santos, F. J.; de Andrade, S. J. *J. Noncryst. Solids* **1999**, *247*, 98.
(15) Park, J.-H.; Oh, C.; Shin, S.-I.; Moon, S.-K.; Oh, S.-G. *J. Colloid Interface Sci.* **2003**, *266*, 107.
(16) Hubert, D. H. W.; Jung, M.; Frederik, P. M.; Bomans, P. H. H.; Meuldijk, J.; German, A. L. *Adv. Mater.* **2000**, *12*, 1286.
(17) McKelvey, C. A.; Kaler, E. W.; Zasadzinski, J. A.; Coldren, B.; Jung, H.-T. *Langmuir* **2000**, *16*, 8285.
(18) Hentze, H.-P.; Raghavan, S. R.; McKelvey, C. A.; Kaler, E. W. *Langmuir* **2003**, *19*, 1069.
(19) Sauer, M.; Streich, D.; Meier, W. *Adv. Mater.* **2001**, *13*, 1649.
(20) Liz-Marzan, L. M.; Giersig, M.; Mulvaney, P. *Langmuir* **1996**, *12*, 4329.
(21) Kamata, K.; Lu, Y.; Xia, Y. *J. Am. Chem. Soc.* **2003**, *125*, 2384.
(22) Emmerich, O.; Hugenberg, N.; Schmidt, M.; Sheiko, S. S.; Baumann, F.; Deubzer, B.; Weis, J.; Ebenhoch, J. *Adv. Mater.* **1999**, *11*, 1299.
(23) Sertchook, H.; Elimelech, H.; Avnir, D. *Chem. Mater.* **2005**, *17*, 4711.
(24) Zoldesi, C. I.; Imhof, A. *Adv. Mater.* **2005**, *17*, 924.
(25) Obey, T. M.; Vincent, B. *J. Colloid Interface Sci.* **1994**, *163*, 454.

10.1021/la060101w CCC: $33.50
Published on Web 03/30/2006

attempts based on a similar approach[26] did not convincingly lead to monodisperse, un-aggregated shells due to difficulties with the silica coating procedure. Instead, our method makes use of copolymerization between the monomers forming the core and the shell. This not only makes the method much simpler to use, but also leads to robust encapsulation of the droplets. The liquid cores can be easily removed, leading to monodisperse, micrometer-sized hollow spherical shells. We find that the shells consist of a cross-linked silica−silicone network, which makes them very elastic. By simply changing the thickness of the shell with respect to the dimension of the core, we obtain three different types of particle, following the same procedure.

In this study, we analyze the influence of the droplet size and the thickness of the coating on the type of particles obtained and the implications for their properties. Furthermore, we discuss the most relevant characteristics of our hollow shells and the possible applications which derive from them.

Experimental Section

Materials. Dimethyldiethoxysilane (DMDES, ≥97.0%) and tetraethoxysilane (TEOS, 98.0%) were obtained from Fluka. 3-Aminopropyl-triethoxysilane (APS, ≥99.0%), fluorescein-isothiocyanate (FITC), and rhodamine B-isothiocyanate (RITC) were purchased from Aldrich and ammonia (29.7 wt % NH_3) and ethanol (absolute alcohol, analytical grade) from Merck. All chemicals were used as received. De-mineralized water was used in all described reactions and also for the cleaning of glassware.

Synthesis. The hollow particles were synthesized using an emulsion templating technique. [24] The two-step fabrication scheme was as follows: silicone oil droplets were first prepared and used as templates for the encapsulation with solid shells. The liquid cores were finally removed by extraction with ethanol. Reactions were performed at room temperature unless stated otherwise.

Oil Droplets. In the first reaction step, monodisperse, stable oil-in-water emulsion droplets, surfactant free, were prepared by hydrolysis and polymerization of the difunctional silane monomer DMDES ($(CH_3)_2Si(OC_2H_5)_2$), following the method described by Vincent and co-workers.[25] The aqueous solutions were prepared using between 1 and 25 volume percent of ammonia (final concentrations of NH_3 between 0.159 M and 3.967 M); different amounts of monomer, in the range of 1−6 volume percent were added, followed by vigorously mixing the reagents for a few minutes. By using different methods of mixing, it was found that this had a noticeable effect on the size of the oil droplets, whereas their monodispersity was much less affected. The droplet sizes corresponding to different mixing methods will be given in the results and discussion section. To obtain reproducible results for the droplet size, most of the samples were prepared using a MS2 minishaker (from Ika), set at maximum speed (2500 rpm).

The emulsion droplets already formed within a few hours, but they were allowed to grow for at least 24 h before the coating step. The emulsions were left without stirring during droplet growth.

Hollow Particles. The encapsulation of the oil droplets with a solid shell was achieved by using a modified version of the classical Stöber procedure.[27] A total of 0.018 M TEOS ($Si(OC_2H_5)_4$) was added to the as prepared emulsion in five steps (5 min between steps) using an Eppendorf pipet, under magnetic stirring. The coating was started 24, 48, or 72 h after the preparation of the oil droplets began, to obtain different thicknesses of the shells. The particles were allowed to complete the shell growth for 3 days. Finally, they were centrifuged and redispersed in ethanol, which was found to penetrate the shells and to dissolve the oil.

Fluorescent Shells. Fluorescent particles were obtained by incorporating RITC dye into the shell during the coating step, using a modified version of the method introduced by van Blaaderen.[28] RITC was first covalently attached to the coupling agent APS by slowly stirring a solution containing 6.5 mg dye and 37.8 mg APS in 1 mL anhydrous ethanol. The reaction was allowed to proceed for at least 12 h by slowly stirring the dye mixture in the dark. Then 0.25 mL of dye solution was added together with 0.018 M TEOS to 400 mL of emulsion, during the encapsulation step, after which the procedure described for the hollow particles was followed.

Characterization. The oil droplets and the hollow particles were analyzed using several methods.

Static Light Scattering (SLS). The size and polydispersity of the oil droplets and the thickness of the coating were determined from SLS measurements, performed with home-built equipment using a He−Ne laser as light source (632.8 nm, 10 mW). Samples were prepared by diluting a few droplets of emulsion with de-mineralized water. The angular distribution of the scattered light was measured at scattering angles in the range $19° \leq \theta \leq 135°$ relative to the transmitted beam, with a photomultiplier tube mounted on a turntable goniometer. The data were plotted against the scattering vector $k = 4\pi n \sin(\theta/2)/\lambda$, where n is the solvent refractive index and λ is the wavelength in vacuum. By comparing the scattering profiles with theoretical ones calculated with the full Mie solution for the scattering factor,[29] the radius and polydispersity were determined. The values for the refractive indices used to fit the experimental data were 1.39 for the oil droplets (corresponding to low molecular weight silicone oil[30]), 1.43 for the solid shells (found by matching their refractive index with dimethylformamide, DMF, which has a refractive index of 1.43), 1.33 for water, and 1.36 for the ethanol.

Nuclear Magnetic Resonance (NMR). Solution ^{29}Si NMR and solid-state ^{29}Si NMR spectroscopy were used to obtain information about the silicon atoms bonded to different groups present in the silicone oil emulsions and in the shell material of hollow spheres, respectively.

^{29}Si NMR spectra in solution were recorded on a Varian Unity Inova spectrometer, at 59.62 MHz with a DEPT (distortionless enhancement by polarization transfer) technique. A value of 7.0 Hz for the Si−H coupling and a θ pulse of 3 μs (27°) were used. The chemical shifts were calibrated vs tetramethylsilane (TMS) in $CDCl_3$ as solvent. Both samples, from a freshly synthesized emulsion (≈10 h old) and an older emulsion (≈4 days since preparation) were prepared by dissolving them in deuterated methanol. In the case of the old emulsion, the oil phase was first separated by centrifugation, and the remaining water was removed using molecular sieves with a pore diameter of 3 Å.

Solid-state ^{29}Si NMR spectra were recorded at 59.62 MHz on a Varian Unity Inova spectrometer equipped with a 7 mm VT CP/MAS probe (CP cross polarization, MAS magic angle spinning). Samples were spun at 5000 Hz in zirconia rotors. Chemical shifts are given in parts per million (ppm), relative to tetramethylsilane; dodecamethylcyclohexasilane ($\delta = -42.0$ ppm) was used as secondary chemical shift reference. In CP/MAS spectra, a contact time of 5 ms and a relaxation delay of 5 s were used. Spectra were averaged from 1616 FIDs. For the solid-state measurements, hollow particles were used, the oil from the core being removed with ethanol; the samples were dried in air, under a heating lamp, for 12 h.

Transmission Electron Microscopy (TEM). The morphology of the different types of shells, after drying, was studied with a Philips Tecnai 12 transmission electron microscope with an accelerating voltage of 120 keV. Samples for TEM were prepared by dipping copper 300 mesh carrier grids covered with carbon-coated Formvar films into dilute suspensions.

Scanning Electron Microscopy (SEM). SEM was also used to study the uniformity of the hollow shells. The micrographs were obtained with a Philips XL 30 FEG scanning electron microscope, and the samples were prepared by drying a drop of concentrated particle suspension on a glass slide.

Energy-Dispersive X-ray Spectroscopy (EDX). The elemental microanalysis of the shell material was achieved by performing

(26) Goller, M. I.; Vincent, B. *Colloids Surf. A* **1998**, *142*, 281.
(27) Stober, W.; Fink, A.; Bohn, E. *J. Colloid Interface Sci.* **1968**, *26*, 62.
(28) van Blaaderen, A.; Vrij, A. *Langmuir* **1992**, *8*, 2921.
(29) Bohren, C. F.; Huffman, D. R. *Absorption and scattering of light by small particles*; John Wiley and Sons: New York, 1983.
(30) Smith, A. L. *The Analytical Chemistry of Silicones*; Wiley-Interscience: New York, 1991.

EDX measurements on a Philips Tecnai 20F high-resolution transmission electron microscope operated at 200 keV, in scanning mode (STEM). The same types of samples as for TEM were used.

Confocal Microscopy. The fluorescently labeled shells were imaged using an inverted Leica confocal scanning laser microscope (CSLM), type TCS-SP2. The microscope was operated in the fluorescence mode. The 543 nm line of a green He−Ne laser was used for excitation of the rhodamine-labeled particles. Measurements were performed with a 100× oil immersion objective with a numerical aperture of 1.4 and a working distance of a 100 μm. The samples were prepared by drying a drop of concentrated dispersion of fluorescent shells on a microscope cover slip of 0.15 mm thickness and 22 mm diameter.

A micrograph of a crystal of capsules in solution was obtained using the following: the bottom of a small glass vial (1.7 mL volume) was replaced by a microscope cover slip (0.15 mm thickness and 22 mm diameter). The cover slip was coated with APS prior use (with a solution of 11.8 vol % APS and 2.2 vol % ammonia (0.36 M NH_3) in ethanol). The vial was filled with a suspension of hollow shells in ethanol (≈1 g/mL), and the particles were allowed to sediment for 2 days during which they formed a colloidal crystal on the bottom. The behavior of the capsules in solution was investigated by operating the microscope in reflection mode, using the 633 nm line. Measurements were performed with a 63× oil immersion objective lens with a numerical aperture of 1.4.

The permeability of the shells was investigated using the same type of special vial as described above, with the bottom replaced by a cover slip. A dispersion of microcapsule-like particles, nonfluorescent, was centrifuged, and the solvent was replaced by ethanol containing 0.725 mM FITC. The sample was imaged in fluorescence mode, excitation line 488 nm, and a 63× oil immersion objective with a numerical aperture of 1.4 was used.

Results and Discussion

Oil Droplets. Low molecular weight poly(dimethylsiloxane) (PDMS) silicone oil-in-water emulsion droplets were synthesized by the base-catalyzed hydrolysis and polymerization of DMDES.[25] These emulsions do not contain a surfactant, but are charge stabilized. The method we use to prepare the emulsions yields monodisperse droplets, with radii in the range of 0.6−2 μm and polydispersities between 3 and 8%. The monomer DMDES is initially insoluble in water, but after a few minutes of mixing (1−4 min, depending of the method), a clear solution is obtained as a result of hydrolysis; within ≈1 h, the solution starts to become milky, indicating the formation of droplets.

To determine which factors influence the oil droplets formation, we prepared emulsions by varying different parameters, such as the monomer and ammonia concentrations, the method of mixing, and the temperature. We found that the droplet size hardly depended on the ammonia concentration in the range 1−25 vol % (0.159−3.967 M NH_3).

However, we observed a strong influence of the mixing procedure. For example, in preparations containing 1 vol % DMDES and 1 vol % ammonia (0.159 M NH_3) in 15 mL total volume of emulsion, we obtained oil droplets of 300−600 nm radius when we used vigorous shaking by hand (1 min), about 700 nm when using the lab-minishaker (2 min, 2500 rpm), and 300−400 nm for shaking by hand (30 s) followed by 5 min of sonication (using a Bransonic 8510 Ultrasonic Cleaner, at 44 kHz). The type of mixing also had a strong influence on the size of the droplets when the total volume of the sample was increased significantly above 30 mL. When larger amounts of emulsions were needed (typically between 100 and 500 mL), the reagents were mixed by vigorously shaking by hand, for 2 min, continuously or intermittent. The size and polydispersity of the droplets obtained were in the same range as for smaller amounts of emulsions but somewhat less reproducible because of the shaking procedure.

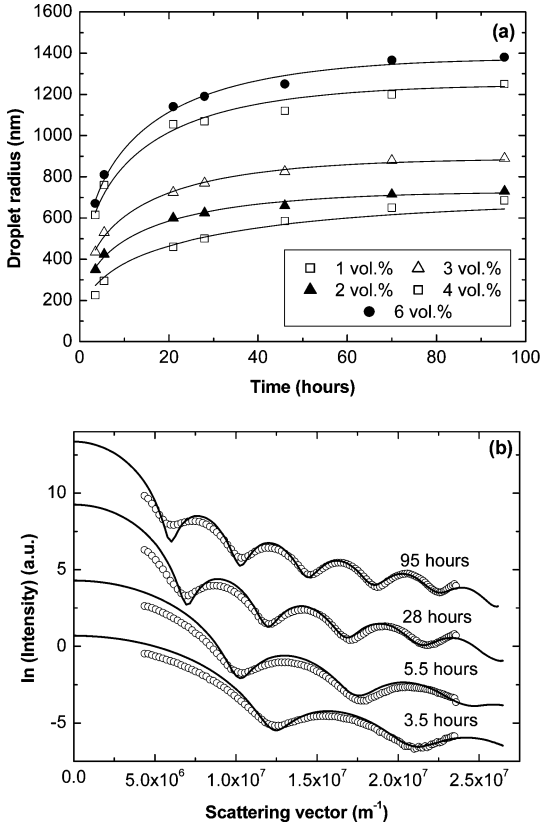

Figure 1. (a) Average droplet radius as a function of time, followed with SLS, for different DMDES concentrations; lines are drawn according to eq 1. (b) SLS experimental data (scatter) fitted by theoretical calculations with full Mie solution of the form factor (lines) for oil droplets prepared from 2 vol % DMDES and 2 vol % ammonia, for different times after preparation; the corresponding radii and polydispersities are as follows: 350 nm and 7% after 3.5 h, 425 nm and 6% after 5.5 h, 625 nm and 4.5% after 28 h and 730 nm and 4% polydispersity after 95 h.

To obtain reproducible results concerning the formation of the oil droplets, we settled on a 4-minute shaking on a lab-minishaker at 2500 rpm, which gave very good results.

Droplet Growth. In one series of experiments, we prepared emulsions varying only the amount of monomer and ammonia used and keeping the rest of the parameters unchanged: 25 mL total volume of the emulsion prepared in a 50 mL glass vial using the lab-minishaker for 4 min at 2500 rpm. We used 1, 2, 3, 4, and 6 volume percent of monomer, and the ammonia concentrations were taken equal with the concentrations of the monomer. By monitoring the radius of the oil droplets over time (Figure 1a), we observed that, even though they are already formed within a few hours, the droplets need about three to four days to reach their final size. After that, their size remains constant, although the larger droplets sometimes begin to coalesce after ≈2 weeks, a problem which can be solved by removing the ammonia by dialysis. Figure 1b shows the experimental scattering data and the theoretical fit for the oil droplets prepared with 2 vol % DMDES and 2 vol % ammonia, for several time intervals after shaking.

In Figure 1a are shown representative results for the growth of the average droplet size. The data can be fitted well by an equation of the form

$$r(t)^3 = r_f^3(1 - \exp(-t/t_1) \qquad (1)$$

where r_f is the final droplet radius. The growth rate of the oil droplets was given by $1/t_1$, where t_1 was used as a fitting parameter.

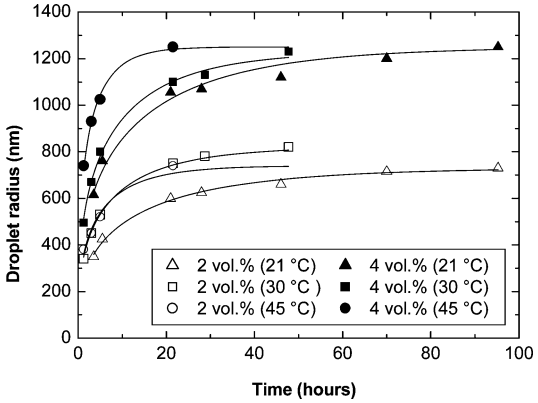

Figure 2. Increase of the droplets radius followed in time, for two monomer concentrations, at three different temperatures (21, 30, and 45 °C). Lines are drawn according to eq 1. Data for samples at 21 °C are the same as presented in Figure 1a for the corresponding DMDES concentrations.

The value for t_1 was found to be 27 ± 2 h for all initial DMDES concentrations, except at 1 vol %, where it was found to be 45 ± 4.5 h. These results suggest that there is a rate limiting step in the condensation reactions, which effectively makes droplet growth a first-order process.

Although the radius of the droplets is clearly influenced by the DMDES concentration, all of the samples show the same behavior in time. The slow increase in droplet size suggests a slow polymerization of the hydrolyzed monomer. Therefore, the desired size of the droplets can be obtained by choosing the amount of monomer used, by varying the time elapsed since the beginning of the synthesis, or both. For all samples, it was observed that the polydispersity is higher in the first hours after the preparation (≈8%), gradually decreases within 24 h (to ≈4%), and hardly fluctuates afterward. These observations regarding the polydispersity exclude Ostwald ripening as a possible late-stage growth mechanism. Therefore, to obtain monodisperse oil droplets (polydispersities better than 5%), at least 20 h should elapse after the mixing of the reagents.

The droplet growth rate could be increased considerably by raising the temperature at which the reaction took place. The same volumes of emulsion were prepared as for the previous experiment, following the same procedure. The concentrations for the monomer used were 2 and 4 vol % respectively. Again, the ammonia concentrations were chosen to be the same as for the monomer. At each concentration, two samples were prepared and kept at different temperatures during the entire experiment: 30 and 45 °C, respectively. The increase in size of the oil droplets was followed in time by taking samples for SLS, and the same eq 1 was used to fit the data. The results are plotted in Figure 2 and compared with those obtained at room temperature (21 °C). The values for the fitting parameter t_1 were found to be smaller for higher temperatures: 16 ± 1 h for both samples prepared at 30 °C, 10 ± 1.5 h for the sample prepared with 2 vol % DMDES at 45 °C, and 5.7 ± 0.2 h for the one with 4 vol % DMDES at 45 °C. This shows that the growth rates ($1/t_1$) increase with increasing temperature. Clearly, the hydrolyzed monomer polymerizes much faster at higher temperatures, but at the same time, the risk of coalescence increases considerably. This happened for samples prepared at 45 °C, already after ≈30 h, and for the ones prepared at 30 °C after ≈50 h, when no more minima were observed in the static light scattering graphs.

Solution ^{29}Si NMR. The suitability of ^{29}Si NMR for determining the structure of silicon containing compounds is well established. Therefore, we used solution ^{29}Si NMR to obtain information about the hydrolysis and condensation products present in PDMS emulsions. Because of the slowness of the reaction, we investigated emulsions at two times after preparation: 10 h old emulsions and emulsions for which the reaction was allowed to complete (4 days).

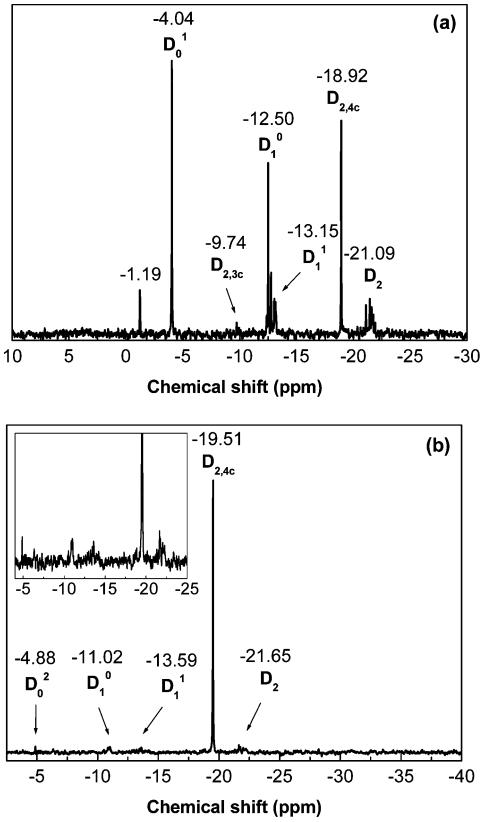

Figure 3. Solution ^{29}Si NMR spectra for PDMS emulsions (a) 10 h old, prepared from 5 vol % DMDES and (b) isolated oil phase ≈4 days after preparation, prepared from 1 vol % DMDES. The inset is a magnification. Subscripts in the peak assignments indicate the number of siloxane groups attached to the site, with "3c" and "4c" denoting sites with three- and four-membered silicon ring, respectively. Superscripts indicate the number of hydroxyl groups, the remaining groups being ethoxy.

Figure 3a presents the spectrum for the 10 h old emulsions, prepared with 5 vol % DMDES and 5 vol % ammonia. The presence of oil droplets in the sample was checked with SLS before the NMR measurement. The sample used for the NMR was taken from the bulk of the oil-in-water emulsion in order to get information about all of the components present in the solution and not only in the droplets.

We were able to identify the resonance lines reported in earlier work[31,32] on base-catalyzed polymerization of DMDES taking place in ethanolic solutions. Throughout this section, the usual D_i^j notation [32] will be used, representing a site with i siloxane bonds and j hydroxyl groups:

$$D_i^j = (CH_3)_2Si(OC_2H_5)_{2-i-j}(OH)_j(O)_{i/2} \qquad (2)$$

Although the emulsion was prepared 10 h before the NMR spectrum was recorded, there is still a significant amount of monomer which is only hydrolyzed at one end (D_0^1), indicated by the strongest resonance in the spectrum at −4.09 ppm. Units having formed a single siloxane bond show up clearly at −12.52

(31) Engelhardt, G.; Jancke, H.; Magi, M.; Pehk, T.; Lippmaa, E. *J. Organomet. Chem.* **1971**, *28*, 293.
(32) Rankin, S. E.; McCormick, A. V. *Magn. Reson. Chem.* **1999**, *37*, S27.

ppm (D_1^0) and −13.2 ppm (D_1^1). The cyclic tetramer (four-membered silicon ring: $D_{2,4c}$), expected for this type of PDMS droplets, is evidenced by the line at −18.89 ppm. Also a small amount of cyclic trimer (three-membered silicon ring: $D_{2,3c}$) units appears at −9.91 ppm. The lines situated at ≈−21.13 ppm correspond to the linear chains connected by two siloxane bonds (D_2). The fact that there are more lines in this region is probably due to the different positions that a unit can occupy in the chain. The line at −1.19 ppm could not be assigned.

Two important aspects are clearly evidenced by the components identified in our spectrum. First, there is already PDMS oil formed 10 h after the emulsion was prepared, indicated by the presence of $D_{2,4c}$, $D_{2,3c}$, and D_2 species; the oil is incorporated in the droplets, their presence being confirmed by SLS performed right before the NMR. Second, most of the DMDES is not yet polymerized, evidenced by the strong lines corresponding to D_0^1 and D_1^0.

The oil droplets already present in the emulsion after 10 h will grow further on account of the large amount of hydrolyzed monomer identified in the sample. This is consistent with the growth of the droplets observed with SLS and sustains the hypothesis of a slow reaction mechanism indicated by the increase of the droplets size in time.

The ^{29}Si NMR spectrum for PDMS emulsions in their final stage is presented in Figure 3b. In this case, the oil droplets have been allowed to grow for 4 days, after which the oil phase was separated by centrifugation. Excess water was removed by using molecular sieves. The spectrum is clearly dominated by the line at −19.51 ppm corresponding to the cyclic tetramer ($D_{2,4c}$), known to be characteristic for this type of emulsions;[25,33] also some linear chains (D_2) were identified by the resonance at −21.65 ppm. The initial DMDES was completely consumed by this time. Interestingly, a small amount of doubly hydrolyzed monomer is still present at −4.88 ppm (D_0^2). Furthermore, traces of hydrolyzed (−13.59 ppm, D_1^1) and unhydrolyzed (−11.02 ppm, D_1^0) end groups were detected. These traces of incompletely condensed units will become part of the encapsulation material, as will be demonstrated shortly.

The studies on the droplet formation show that the silicone oil droplets prepared by hydrolysis and polymerizations of DMDES are excellent candidates for templating with a solid silica based shell because of several reasons. First of all, their monodispersity and size within the micrometer range makes them suitable templates for colloidal core−shell particles. Second, the slow reaction course of their formation allows us to choose the desired size of the cores and the amount of nonpolymerized DMDES present in the sample when starting the coating step and which will copolymerize together with TEOS to form the solid shells. Finally, but equally important, the silicone oil obtained is of a low molecular weight,[33] which makes it easy to remove in the final step of the synthesis.

Hollow Particles. The silicone oil droplets described in the previous section were used as templates for encapsulation with a solid shell.[24] The coating was achieved by hydrolysis and condensation of tetraethoxysilane, which was added to the as prepared emulsions during magnetic stirring, in five steps (5 min between steps). Surprisingly, we found that the thickness of the coating did not depend on the amount of TEOS added. Instead, the time elapsed between the beginning of the emulsion preparation and the addition of TEOS was found to be the decisive factor in the final thickness of the shell, with the thickness increasing as TEOS was added sooner. Moreover, the thickness of the coating often exceeded the maximum thickness expected from the amount of TEOS used: when the encapsulation step was started between 24 and 48 h after the beginning of the emulsion preparation, the expected value for the shell thickness based on the amount of TEOS added represented only 10−20% of the shell thickness measured with SLS. Apparently, the unreacted DMDES monomer still present in the emulsion during the encapsulation process contributes significantly to the shell growth. For a given size of the droplets, the more time elapses between the droplet formation and encapsulation, the less monomer is left and the thinner the resulting shell. This is a direct result of the slow polymerization of the monomer, as discussed in the previous section.

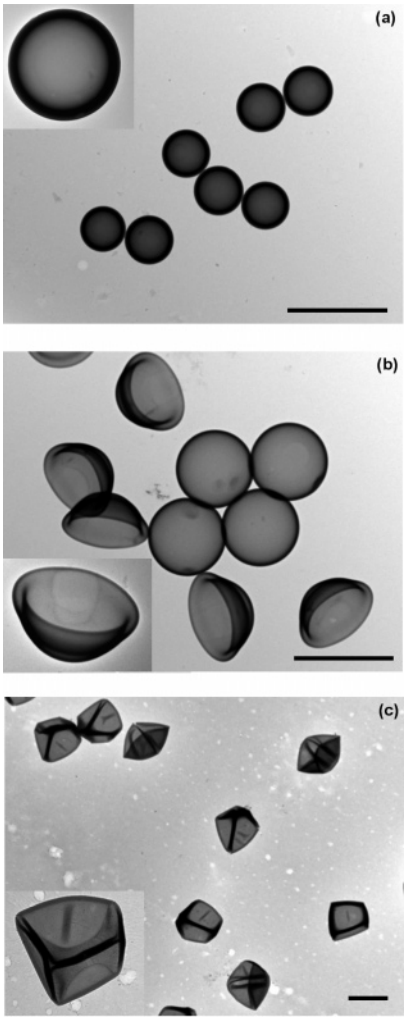

Figure 4. TEM micrographs of hollow particles: (a) microspheres (core radius 420 nm, shell thickness 150 nm, 7% polydispersity), (b) microcapsules (core radius 795 nm, shell thickness 150 nm, 3% polydispersity), and (c) microballoons (core radius 1065 nm, shell thickness 10 nm, 4% polydispersity). The size and polydispersity obtained from SLS, scale bars 2 μm.

Typical TEM images of these particles are shown in Figure 4. Based on the way in which the particles collapse upon drying, we distinguish three types of hollow spheres: microspheres (a), microcapsules (b), and microballoons (c). The microspheres remain undeformed as a result of drying; the microcapsules, more flexible and deformable, collapse, forming hemispherical, double-walled caps, whereas the microballoons have a crumpled appearance. The deformation took place upon drying a sample for TEM. In solution, on the contrary, all coated droplets were

(33) Neumann, B.; Vincent, B.; Krustev, R.; Muller, H.-J. *Langmuir* **2004**, *20*, 4336.

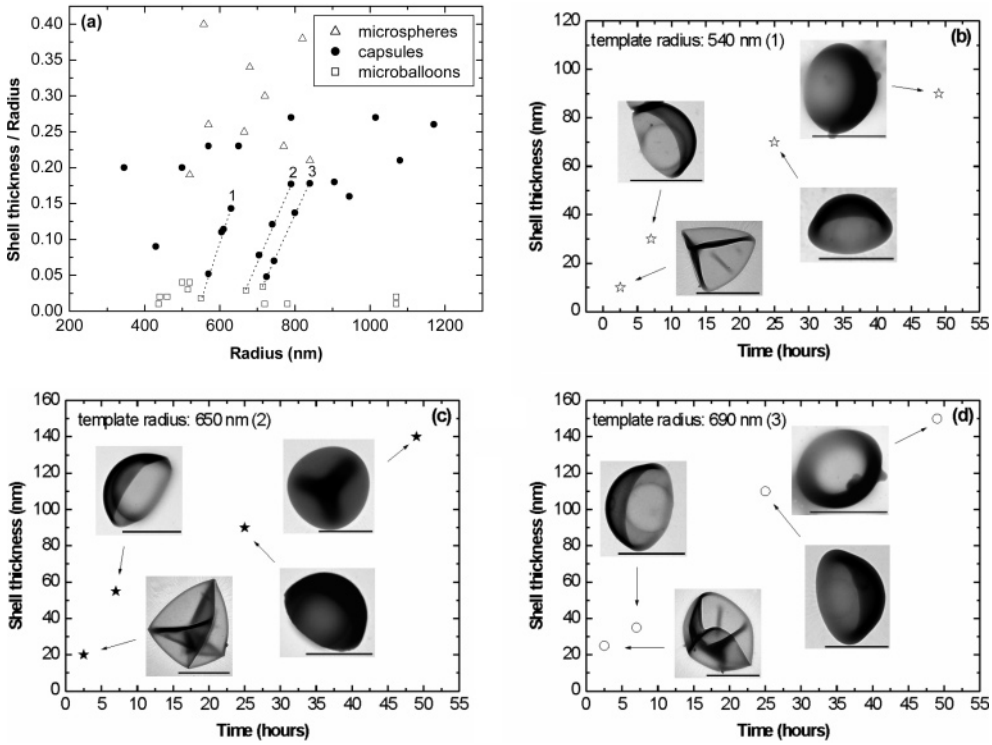

Figure 5. (a) Diagram showing the types of particles corresponding-to-different ratios between the shell thickness and the total radius of the particle: triangles-microspheres, circles-capsules and squares-microballoons. Lines 1, 2 and 3 connect points belonging to three samples for which the growth of the shell was followed in time: (b) line 1, template radius 540 nm, (c) line 2, template radius 650 nm, and (d) line 3, template radius 690 nm. Scale bars for TEM images: 1 μm.

found to remain spherical. This was seen by optical microscopy and also from the fact that the SLS data still showed well-defined minima characteristic for (coated) spheres. Representative SLS data have been published in ref 24. These SLS experiments allowed us to obtain an accurate measurement of the coating thickness, which agreed well with the values obtained from the analysis of TEM images.

The microspheres (Figure 4a) were obtained by adding 0.018 M TEOS, under magnetic stirring, to 200 mL of emulsion prepared 24 h earlier from 1 vol. % DMDES and 10 vol % ammonia in water at room temperature. For the microcapsules (Figure 4b), oil droplets synthesized using the same concentrations of monomer and ammonia (but in 400 mL total volume) were coated with a solid shell by adding 0.018 M TEOS after 48 h since the emulsion preparation. In both cases (microspheres and microcapsules), the shell was allowed to grow for 3 days after the addition of TEOS. This was necessary because, as mentioned earlier, the monomer contributes significantly to the shell thickness and its polymerization is rather slow. The third type of particles, microballoons, were obtained by coating oil droplets (prepared in 25 mL emulsion, 5 vol % DMDES, 5 vol % ammonia) with a solid shell by adding 0.018 M TEOS after 72 h after their preparation.

The shell thickness for the microspheres and microcapsule-like particles was found to vary between 50 and 300 nm, whereas for the microballoons, it never exceeded 30 nm. Yet, the important parameter in distinguishing the three types was the shell thickness (d) relative to the total radius (R) of the particle. This is seen from Figure 5a which gives an overview of the different types of particles for different values of d/R.

For high values of this ratio, the hollow shells maintain their spherical shape after drying. This is the case for microspheres, situated in the upper part of the diagram in Figure 5a, for values of $d/R > 0.23$. When the ratio becomes smaller (0.05−0.25), we observed a collapse of the spherical shells, forming hemispherical caps. The lower region of the diagram contains the microballoons, even more deformable shells which collapse showing creases and folds, as a result of their very thin shells ($d/R < 0.05$). As can be seen in Figure 5a, the boundary between two neighboring regions is not perfectly sharp. Close to the transition regions, particles of both types can be found in the same sample.

These results clearly show that the main factor determining the shells deformation is the ratio d/R. This can be understood from elasticity theory, which predicts that the pressure difference needed to indent a hollow ball should be proportional to $(d/R)^2$.[34,35] The origin of this pressure difference probably lies in the occurrence of capillary forces during drying.

A very interesting and potentially useful aspect of Figure 5a is that, for the same size of the template, different types of particles can be obtained by tuning the shell thickness. Conversely, for a given shell thickness, the behavior of the particle can be varied by suitably choosing its radius.

The growth of shells corresponding to the lines 1, 2, and 3 from Figure 5a is presented in Figure 5b−d, and it shows the flexibility of our method in tuning the types of hollow particles. Due to the slow condensation of the monomer, the shell thickness increases gradually, and as a result, the particles behavior will change continuously until the growth is completed. Consequently, microballoon-like particles are obtained after a few hours (≈2.5 h), which evolved to microcapsules with thicker and thicker shells. Although the final shells were quite thick for all three samples, the particles still behaved like microcapsules because the final ratio between the shell thickness and their total radius was just below 0.25 (see Figure 5a). The reaction can be stopped

(34) Landau, L. D.; Lifshitz, E. M. *Course of Theoretical Physics, Vol.7, Theory of Elasticity*, 3rd ed.; Butterworth-Heinemann: Oxford, 1997.

(35) Pogorelov, A. V. *Bending of Surface and Stability of Shells*; American Mathematical Society: Providence, RI, 1988.

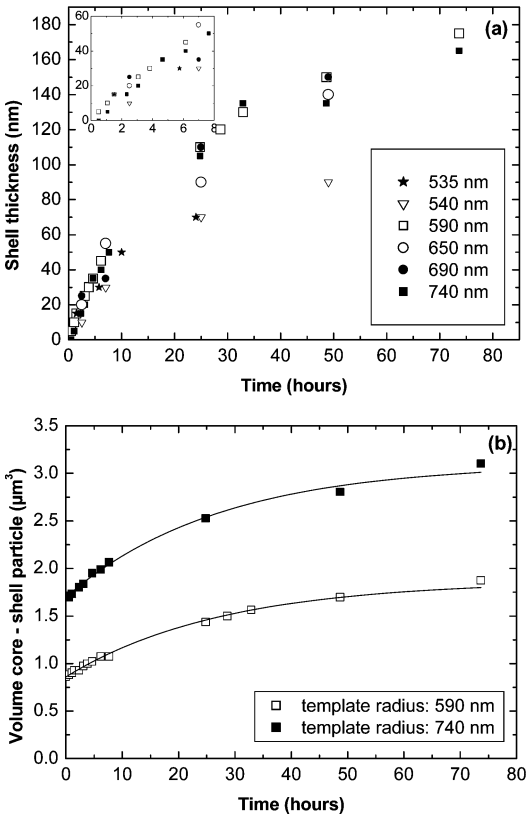

Figure 6. (a) Increase of the shell thickness followed in time, for different radii of the template as indicated in the legend. Inset shows the growth within the first 8 h after TEOS was added. (b) Average particle volume as a function of time, for two different template size; lines are drawn according to eq 3.

at any time (either by dialysis or centrifugation), depending on what type of particles are needed. Consequently, we have two ways of obtaining the desired hollow shells: either by choosing the time when the coating is started and allowing the reaction to proceed to the end or by monitoring the shell thickness and stopping the reaction when satisfied with the shell thickness.

As pointed out above, the shell thickness is directly related to the amount of DMDES left in the sample during the encapsulation step. This means that the shell should grow in time at a similar rate as the oil droplets. Indeed, by following the shell thickness in time (Figure 6a), for different size of oil droplets used for encapsulation, we observed a significant growth for a relatively long period of time. All of these samples were prepared by adding 0.018 M TEOS to the emulsions prepared with 2 vol % monomer and 2 vol % ammonia, except for one (the sample with 740 nm droplet radius was prepared from 3 vol % DMDES, 3 vol % ammonia). The coating was started in all of these cases after 24 h since the emulsion synthesis began.

The evolution of the shells within the first hours (inset in Figure 6a) can be characterized as a reaction-limited growth process[36] since the growth rate of the shell thickness is found to be independent of the radius of the template. The overall growth of the coated particles is governed by the same growth rate as found for the oil droplets. This is seen in Figure 6b which shows the increase in volume of the coated droplets, for two different templates. The change in total radius of the coated droplet takes the form

$$R(t)^3 = R_f^3 - (R_f^3 - R_0^3)\exp(-t/t_1) \qquad (3)$$

where R_f represents the final particle radius and R_0 the radius of the template which remains constant during the encapsulation. The fitted growth rate $1/t_1$ has precisely the same value as found for the emulsion droplets ($t_1 = 27 \pm 2$ h). This is evidence for our conclusion that the shell growth is less influenced by the TEOS and relies more on the presence of hydrolyzed DMDES and that the latter determines the growth rate through a rate-limiting step which is effectively first order.

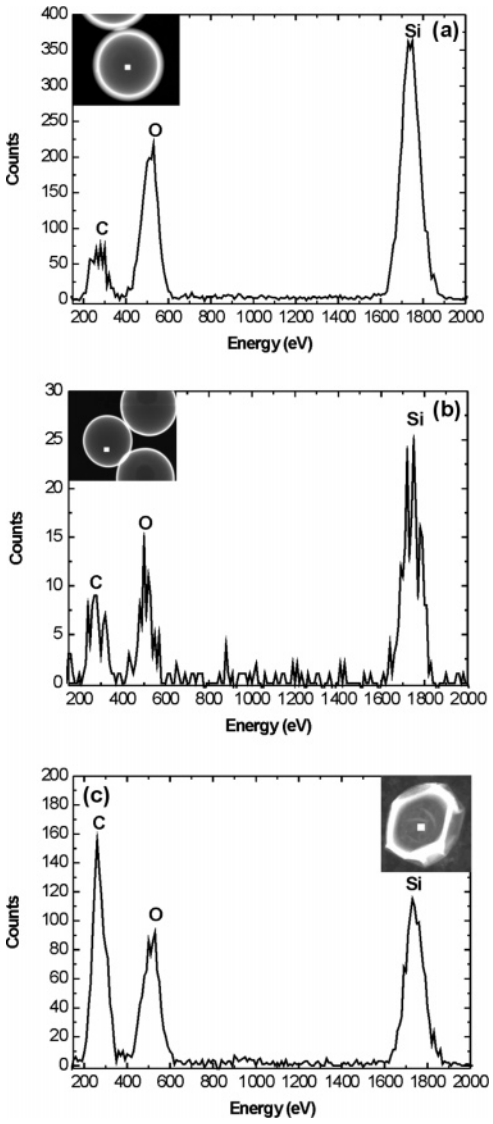

Figure 7. EDX spectra recorded in the middle of the particles, in the points indicated by the white squares from the insets (representing TEM dark field images) for (a) microsphere, (b) microcapsule, and (c) microballoon.

EDX Analysis. The large contribution of siloxane units to the shells can be seen in EDX elemental microanalysis on samples in which the liquid cores had been removed by washing in ethanol and drying (Figure 7).

Differences among the samples are seen by comparing the relative ratios Si/O and Si/C for all types of shells. The Si/O ratio remains almost the same for all three particles, whereas the Si/C ratio decreases in going from microspheres to microcapsules and microballoons. The increase in carbon content relative to silicon implies a larger proportion of dimethylsiloxane units in the shell material.

(36) van Blaaderen, A.; van Geest, J.; Vrij, A. *J. Colloid Interface Sci.* **1992**, *154*, 481.

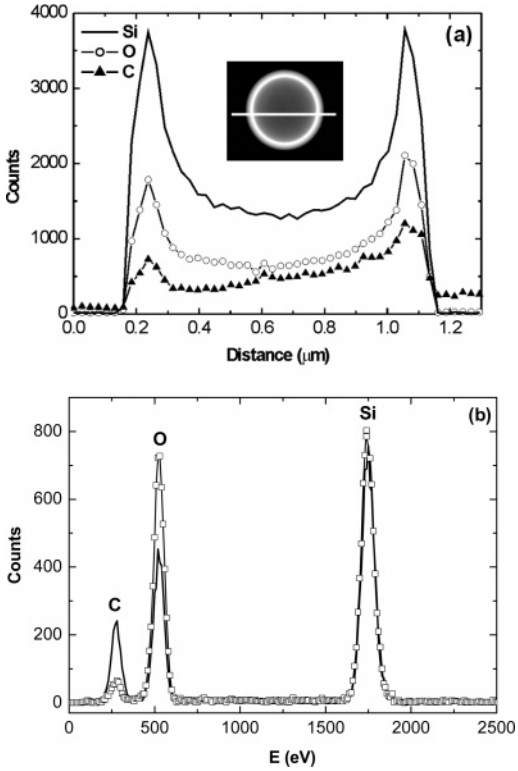

Figure 8. (a) EDX line graph acquired in STEM mode, from a line scan (white line) through the microsphere showed in the inset (TEM dark field image). (b) EDX line spectrum recorded in the middle of the shell of a microsphere, before (line) and after (line + scatter) calcination in air at 500 °C for 4 h.

The EDX line scan on a microsphere presented in Figure 8a indicates the hollow structure of the particles, as well as the shell composition, rich in carbon because of the DMDES contribution.

As already shown, because of their thick shell relative to their radius, the microspheres maintain their spherical shape after drying. Moreover, their shell can sustain calcination at high temperatures (500 °C) without their structure being affected. The changes in their composition were determined by performing EDX analysis of the shell material before and after calcination: they indicated that the carbon was replaced by oxygen during the calcination in air, as shown in Figure 8b. The remaining carbon signal after calcination is due to the carbon-coated sample grids, which also causes the nonzero baseline in Figure 8a. Thus, the hybrid silica/siloxane shell can be converted to pure silica by calcination.

^{29}Si Solid-State NMR. The chemical structure of the shell material was determined from ^{29}Si solid-state CP/MAS NMR spectra. The hollow shells used for these measurements were obtained by adding 0.018 M TEOS to an emulsion prepared from 1 vol % DMDES and 10 vol % ammonia and subsequently removing the oil from the core by transferring the coated droplets in ethanol. The resulting hollow shells were dried in air, under a heating lamp, for 12 h prior the measurements. This treatment completely removes the liquid cores. The ^{29}Si NMR spectrum is shown in Figure 9.

A silicon atom bonded through siloxane bonds (O−Si) with four other silicons is designated as Q_4. A silicon atom with three O−Si bonds is named Q_3. They are usually found in silica particles [13,37] obtained from TEOS following the Stöber procedure. [27] The presence of Q_4 in our spectrum is indicated by the relative strong resonance situated at −109.13 ppm; there is also a trace of Q_3 (−99.60 ppm). However, the strongest line in the spectrum belongs to the cyclic tetramer ($D_{2,4c}$)[38,39] consisting of di-functional units, built into cyclic tetramers containing also one or more Q_4 units from the TEOS. Such a structural unit is represented in Figure 10, with Si* indicating silicon atoms in di-functional units. Upon copolymerization of mixtures of DMDES and TEOS, the region of −11 to −14 ppm has been shown to contain the signals from dimers and end groups of linear oligomers,[38,39] which can explain the appearance of the shoulder situated at the left side of $D_{2,4c}$. It has been previously reported[38,39] that TEOS can indeed act as the linking unit between cyclic oligomers.

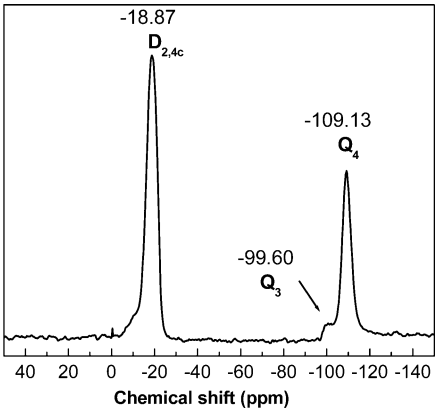

Figure 9. ^{29}Si CP NMR spectrum of hollow shells (core radius: 735 nm, shell thickness: 280 nm). By Q_3, Q_4 are designated silicon atoms bonded with three or four other silicon atoms, respectively and $D_{2,4c}$ represents a cyclic tetramer.

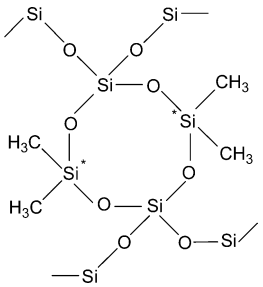

Figure 10. Cyclic tetramer ($D_{2,4c}$) consisting of di-functional units (silicon atoms in these units indicated by Si*) coming from the DMDES, cross-linked with tetra-functional units from the TEOS.

Thus we conclude that our shells consist of a cross-linked silicate/siloxane network, in which TEOS plays the role of cross-linker. This explains why a major contribution to the shell comes from the DMDES and why the shell thickness is mainly determined by the amount of DMDES left in the emulsion.

Fluorescent Shells. The properties of concentrated suspensions of hollow particles can be studied by confocal scanning laser microscopy (CSLM), if fluorescent dyes are incorporated in their shells. Therefore, to achieve fluorescence in our systems, we used a modified version of the procedure to incorporate dyes through covalent bonds into colloidal silica spheres described previously.[28] The procedure consists of two steps. First, the dye RITC was chemically bound to the silane coupling agent APS, and second, the dye mixture was added to the emulsion, together with TEOS, during the encapsulation step; the fluorescent dye ended up chemically incorporated in the particle shell. An example of dye-functionalized hollow shells is presented in Figure 11, showing that the shells were successfully labeled. As an alternative, the dye RITC can be replaced by FITC which can

(37) van Blaaderen, A.; Vrij, A. *J. Colloid Interface Sci.* **1993**, *156*, 1.
(38) Brus, J.; Dybal, J. *Polymer* **1999**, *40*, 6933.
(39) Brus, J.; Dybal, J. *Polymer* **2000**, *41*, 5269.

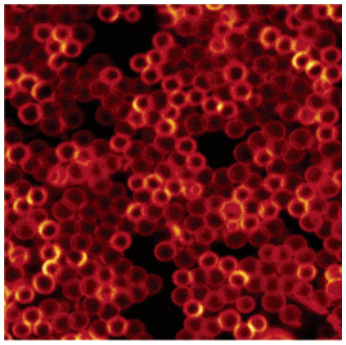

Figure 11. Confocal microscopy image (fluorescence mode $\lambda =$ 543 nm, image size: 23 μm $\times$ 23 μm) of hollow fluorescent shells (core radius 800 nm, shell thickness 100 nm) dried on a microscope cover slip.

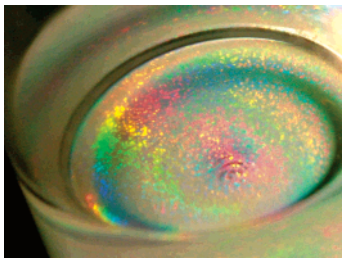

Figure 12. Photograph of a crystal of capsules sedimented in ethanol (core radius 795 nm, and shell thickness 150 nm).

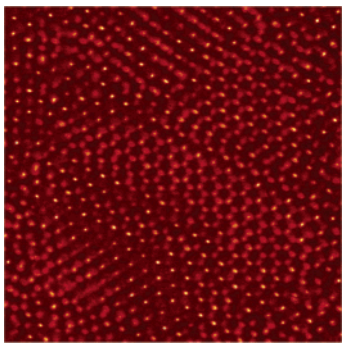

Figure 13. Confocal image (reflection mode, $\lambda =$ 633 nm) of capsules (core radius 795 nm, shell thickness 150 nm) sedimented in ethanol. Image size: 43 μm $\times$ 43 μm.

be chemically incorporated into the shell by using the same procedure described above.

Fluorescent particles can be also obtained by simply adding RITC dissolved in ethanol or water (depending of the solvent in which particles are dispersed), to the suspension of particles (final RITC concentration $\approx$4.4 $\times$ 10^{-3} mg/mL). In this case, the dye will be adsorbed at the surface of the particles but can be washed away any time by changing the solvent. The FITC dye cannot be used in the latter method because, instead of being adsorbed at the surface, it penetrates the shell.

Crystallization. Because of their high uniformity in size, the hollow shells are able to form colloidal crystals. Although the microcapsule-like particles collapse when dried, in solution they are spherical and sediment on the bottom of the vial, giving rise to colorful Bragg reflections, as shown in Figure 12.

The crystal structure formed by the capsules in solution was investigated by confocal microscopy. Figure 13 shows an image in reflection mode of the bottom layer of a crystal of hollow spheres (core radius 795 nm, shell thickness 150 nm), sedimented in ethanol. The distance between the centers of two neighboring particles was found to be $\approx$2.2 μm, somewhat larger than the particle diameter (1.89 μm), because of a surface charge of the particles and low concentration of salt.

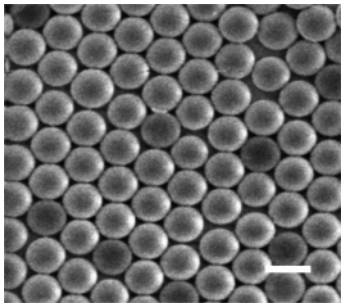

Figure 14. SEM image of a dried crystal of hollow microspheres (core radius 420 nm, shell thickness 150 nm). Scale bar 2 μm.

As already shown, the microspheres maintain their spherical shape even after drying; therefore they can form dry colloidal crystals similar to those of solid silica spheres. An example of a crystal of hollow microspheres is given in Figure 14, and it was obtained by drying a suspension of hollow particles (core radius 420 nm and shell thickness 150 nm) in ethanol, on a microscope cover slip.

The microballoon-like particles are highly deformable because of their extremely thin shells. However, when packed and dried, they form highly porous materials with a large volume of voids, which open an entirely different range of applications.

Shell Permeability. As mentioned above, the dissolution of the particle core is possible by using ethanol, which penetrates the shells and dissolves the PDMS oil. This already implies shell porosity sufficiently high for small molecules to pass through. Additionally, we investigated the shell permeability more thoroughly with confocal microscopy.

Several qualitative experiments were performed using different capsule-like particles and fluorescently labeled solvents. The experiments proceeded as follows: hollow shells, nonfluorescent, dispersed in ethanol, were allowed to sediment, and the solvent was replaced by ethanol containing 0.725 mM FITC; these dispersions were put in the special vials described in the Experimental Section and imaged in fluorescence mode. The ethanol with FITC was found to penetrate the shells, and as a result, fluorescence is observed also from inside the particles (Figure 15a).

Taking into account the size of the FITC molecule (the longest distance 1.12 nm), the pores of the shell should be at least 1.1 nm in diameter to allow the dye to enter the particle. Subsequently, after the particles had sedimented on the bottom of the vial, the ethanol containing FITC was replaced by fresh ethanol. The fluorescence from the particle cores could still be observed within the first minutes after changing the solvent (Figure 15b); subsequently, it diffused out, being replaced by clean ethanol. The particles in Figure 15b appear deformed, but this is due to flow resulting from mixing in the fresh ethanol.

The release of the ethanol with FITC from the microcapsules is captured in close-up in Figure 15c. The hollow shells were first dispersed in ethanol containing the same dye concentration as before; subsequently, they were quickly filtered and immediately resuspended in clean ethanol. A glass capillary (0.1 $\times$ 2.0 mm) was filled with the new suspension and imaged in fluorescence mode. The particles appear to have "tails" because the FITC diffusing out of the shells is carried off by the residual flow in the sample.

Although the experiments with fluorescent tracers were just qualitative, they demonstrate the permeability of the shells and the opportunity of refilling these microcapsules with different

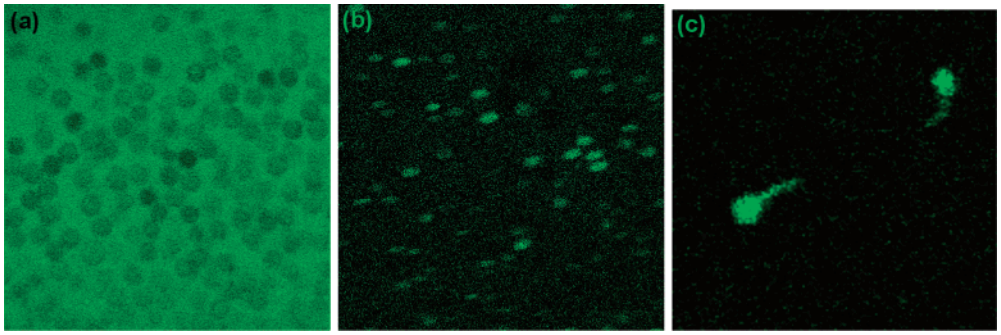

Figure 15. (a) Confocal image (fluorescence mode, $\lambda = 488$ nm) of microcapsule-like particles (core radius 795 nm and shell thickness 150 nm), dispersed in ethanol containing 0.725 mM FITC and (b) images taken after the solvent had been quickly replaced with clean ethanol, during scanning, after 40 s. Images size: 29.8 μm $\times$ 29.8 μm. (c) Confocal image (fluorescence mode, $\lambda = 488$ nm) illustrating the release of the ethanol with FITC from capsule-like particles (core radius 850 nm and shell thickness 230 nm) dispersed in ethanol, $\approx$4 min after they were resuspended in clean ethanol. Image size: 23.3 μm $\times$ 23.3 μm.

chemicals. This opens the possibility of using them as microreactors or controlled release agents.

Conclusions

As shown by our investigations, the emulsion templating technique is a suitable approach for preparing hollow colloidal particles with tunable properties. Because of the relatively slow reaction, the PDMS oil droplets obtained from hydrolysis and polymerization of dimethylsiloxane monomer are excellent templates for encapsulation with solid shells using tetraethoxysilane. Their size can be controlled not only by the amount of monomer used but, more importantly, also by the time between preparation of the emulsion droplets and addition of the encapsulating material. The monodispersity of the emulsion droplets is an important characteristic for their use as templates. Furthermore, the low molecular weight silicone oil obtained can be easily dissolved in ethanol after the droplets have been encapsulated with a solid shell. The polymerization of DMDES limits the reaction rate both for oil droplet growth and shell growth.

Hollow colloidal particles in the micrometer range can be prepared by starting with these oil droplets as templates, using a straightforward synthesis. Our technique allows us to prepare variable shell thicknesses, from 10 to 300 nm in a simple two-step process. The shells consist mainly of dimethylsiloxane units cross-linked with tetrafunctional silicate units, as shown by ^{29}Si NMR and EDX analysis.

The deformation of the particles depends only on the ratio between the shell thickness and the particle radius; therefore, by simply tuning this ratio, three different types of particles can be obtained, with different properties and different perspectives for applications. Due to the specific reaction kinetics, this ratio can be selected either by varying the time between the preparation of the emulsions and the start of the coating step or by interrupting the encapsulation reaction.

The incorporation of fluorescent dyes into the shells opens up the possibility of investigating concentrated suspensions of such particles using confocal microscopy.

As we already illustrated, a direct consequence of the monodispersity of our hollow shells is that they may have applications in making ordered materials, either crystalline or porous microcellular structures. The shells permeability for small molecules is an indication of their possible use in microencapsulation and as microreactors. Variation of the shell thickness provides a simple means for controlling the permeability.

Clearly, these hollow colloidal particles have perspectives as precursors for fabrication of various materials, the flexibility of their synthesis being an important advantage.

Acknowledgment. We thank J. D. Meeldijk for EDX, C. M. van Kats for SEM, J. H. J. Thijssen for Mathematica notebooks, and A. van Blaaderen and C. Quilliet for helpful discussions. This work was financially supported by the Nederlandse Organisatie voor Wetenschappelijk Onderzoek (NWO).

LA060101W